Stabilization of large drainage basins over geological timescales: Cenozoic West Africa, hot spot swell growth and the Niger River

Dominique Chardon, Jean-Louis Grimaud, Delphine Rouby, Anicet Beauvais, Frédéric Christophoul

Stabilization of large drainage basins over geological timescales: Cenozoic West Africa, hot spot swell growth and the Niger River

Dominique Chardon[1*], Jean-Louis Grimaud [2,3,4], Delphine Rouby[2], Anicet Beauvais[5], Frédéric Christophoul[3]

[1] IRD, UMR 234, GET, 14 avenue Edouard Belin, 31400 Toulouse, France

[2] CNRS, GET, 31400 Toulouse, France

[3] Université de Toulouse, UPS (OMP), GET, 31400 Toulouse, France

[4] Now at St Anthony Falls Laboratory, University of Minnesota, 2 Third Avenue SE, Minneapolis, MN 55414, USA

[5] Aix Marseille Université, IRD, CNRS, CEREGE UM34, BP 80, 13545 Aix en Provence Cedex 4, France

Submitted to G-Cubed, 4 November 2015

Revised, 27 January 2015

* Corresponding author
Email: dominique.chardon@ird.fr; Tel: 33 5 61 33 25 70, Fax: 33 5 61 33 25 60

Abstract – Reconstructing the evolving geometry of large river catchments over geological timescales is crucial to constraining yields to sedimentary basins. In the case of Africa, it should further help deciphering the response of large cratonic sediment routing systems to Cenozoic growth of the basin-and-swell topography of the continent. Mapping of dated and regionally correlated lateritic paleolandscape remnants complemented by onshore sedimentological archives allows the reconstruction of two physiographic configurations of West Africa in the Paleogene. Those reconstructions show that the geometry of the drainage stabilized by the Late Early Oligocene (29 Ma) and probably by the end of the Eocene (34 Ma), allowing to effectively link the inland morphoclimatic record to offshore sedimentation since that time, particularly in the case of the Niger catchment – delta system. Mid-Eocene paleogeography reveals the antiquity of the Senegambia catchment back to at least 45 Ma and suggests that a marginal upwarp forming a continental divide preexisted Early Oligocene connection of the Niger and Volta catchments to the Equatorial Atlantic Ocean. Such a drainage rearrangement was primarily enhanced by the topographic growth of the Hoggar hot spot swell and caused a major stratigraphic turnover along the Equatorial margin of West Africa.

1. Introduction

Reconstructing the evolving geometries of large drainage basins over geological time scales (10^6-10^7 yr) is key to linking the sediment routing system to the deformation and landform evolution processes of continents. It is also crucial to constrain clastic sedimentary fluxes towards sedimentary basins. Along passive continental margins, stratigraphic architectures and sedimentary records would indeed be primarily sensitive to inland catchment size and therefore to drainage rearrangement (e.g., Rouby et al.,

2009). But conversely, the sedimentary record in itself may not be used as an unequivocal proxy of change in inland drainage given the multiplicity of factors controlling sedimentation and their interactions. The drainage of the African continent has evolved with the growth of a continental-scale basin-and-swell relief (Fig. 1), which results from the interplay of marginal upwarps sustained or rejuvenated since Gondwana continent break-up and intraplate Cenozoic hot spot swells (Burke, 1996; Summerfield, 1996). Within such an evolving topographic framework that is still poorly constrained, the age and acquisition mode of the main river courses remain controversial. Key questions are to know whether, when, and how short coastal rivers became connected to large inland drainage basins (Summerfield, 1996). Solving those questions is particularly relevant for interpreting the increase of clastic sediment fluxes around the African continent following Eocene peak greenhouse and its links with lithospheric deformation (Séranne, 1999; Burke et al., 2003).

A large body of research exists on river network evolution of numerous drainage basins of the African continent. Inland deltas, elbows and steps (knickzones and knick points) along river courses have been considered as recording rapid headward erosion by coastal rivers having "recently" captured inland drainages via piracy (e.g., Goudie, 2005). Such interpretations are solely based on the present day geometry of river networks and topography. At best, much ambiguity therefore remains on drainage reorganization scenarios given the paucity of evidence for past river courses and their age (Summerfield, 1996). The high steepness and stepped character of modern African rivers' lower reaches may be interpreted as a consequence of the maintenance of rivers across continental margins during continental uplift (e.g., Bond, 1979; Burke, 1996). Alternatively, models of denudational isostatic uplift of the seaward slope of marginal upwarps suggest maintenance of dual (inland and seaward) drainage systems long after

rifting (Summerfield, 1985; Gilchrist and Summerfield, 1990). Such a configuration would lead steep aggressive costal rivers to eventually capture the interior drainage (Gilchrist et al., 1994; Summerfield, 1996). In order to test these interpretations, arguing either for antiquity or youthfulness of the drainage, geological markers documenting past drainage configurations are required.

Here we investigate the Cenozoic drainage development of West Africa (Fig. 2) by mapping dated and regionally correlated lateritic paleolandscape remnants that are widely and densely distributed over the sub region. This allows reconstructing two Paleogene stages of the West African paleogeography showing that the main river courses of the sub region stabilized since at least the Latest Early Oligocene (~29 Ma). This result opens new perspectives on linking the continental geomorphic record to the sedimentary evolution of the Equatorial margin of Africa. We also document the key role of the growth of the Hoggar hot spot swell in reorganizing the relief regionally and leading to the installation of the modern drainage.

2. Regional context and earlier works

The drainage of West Africa is organized around three topographic massifs: the Guinean Rise forming the continental divide the closest to the coast and the Hoggar and Jos Plateau Cenozoic hot spots (Fig. 2). Rivers directly flowing to the Atlantic Ocean are increasingly longer to the east of the Guinean Rise, the continental divide being located ~1400 km from the coast at the northernmost headwaters of the Volta river system (Fig. 2). The Niger River catchment may be divided in three sub-drainage areas. The main area drains mostly the Hoggar swell and the Jos plateau. The High Niger catchment is NE-trending and comprises the drainage upstream the elbow in the river course. The Benue River catchment constitutes the third sub-drainage area (Fig. 2). The

105 Gambia and Senegal catchments fringe the northwestern watershed of the High Niger
106 and flow towards the Central Atlantic Ocean (Fig. 2). The High Niger and Sourou
107 inland deltas are large functional inland alluvial plains (Fig. 2).
108 Since exploration by Chudeau (1909), the elbow between the High and Low
109 Niger (Fig. 2) has been considered to result from a Quaternary capture of the inland
110 delta, which would have been drained by river(s) flowing north- or northwestward into
111 the Taoudeni basin or the Hodh depression until capture by the Low Niger (Chudeau,
112 1919; Furon, 1929, 1932; Urvoy, 1942). But neither sediment accumulations nor paleo-
113 river courses exist that would support the existence of such rivers (Beaudet et al.,
114 1977a). The delta was interpreted to result from damming of the High Niger River by
115 Late Quaternary sand dunes and Urvoy (1942) and Tricart (1959) favored "very recent"
116 aggradation-driven overspill to explain its connection to the Low Niger. However,
117 Beaudet et al. (1981a) argued that the delta has used a persistent spillway at the location
118 of its current downstream sill. Other authors such as Voute (1962) inferred a recent
119 Quaternary connection between the Lowermost Niger River and the rest of the Niger
120 catchment upstream its confluence with the Benue (Figs. 1 and 2). According to Hubert
121 (1912) and Palausi (1959), the Sourou delta (also known as the Gondo plain, Fig. 2) was
122 formed by the Sourou River that flowed northeastward into the Low Niger before its
123 connection to the Volta drainage in the Latest Quaternary.
124 The prevailing view on the West African river network, and particularly the
125 Niger, is therefore that of a youthful drainage resulting from Quaternary
126 rearrangement(s). This view is still deeply entrenched in the literature (Goudie, 2005)
127 although it remains largely conjectural due to the lack of geological markers of past
128 river courses and in absence of age constraints on such markers. Recent advances made
129 by dating (Beauvais et al., 2008) and mapping remnants of a unique sequence of

130 spatially correlated Cenozoic lateritic incision markers at the scale of West Africa
131 (Beauvais and Chardon, 2013; Grimaud et al., 2014) offer an opportunity to test the age
132 of the drainage and its potential evolution on the Cenozoic timescale.
133
134 **3. Lateritic paleolandscape markers and field investigations**
135 The present day topography of West Africa results from the dissection of the
136 African Surface, a landscape being the product of a protracted period of lateritic
137 weathering that culminated and ended during Eocene peak greenhouse (Boulangé and
138 Millot, 1988; Beauvais and Chardon, 2013). Remnants of this landscape bear thick (>
139 80 m) bauxite-capped weathering profiles, which are preserved throughout West Africa
140 as mesas (Fig. 3) defining the topographic envelope of the sub region. Lateritic bauxites
141 developed on all pre-Cenozoic rocks exposed in West Africa during the Paleocene and
142 Eocene. Stratigraphic and sedimentologic investigations have established the
143 synchronicity and link between inland bauxite production and Early to Mid-Eocene
144 marine chemical sedimentation in the basins of the sub region. This allowed
145 constraining a stratigraphic age for the bauxites (Millot, 1970) and correlating the
146 African surface with Paleogene marine series now buried in those basins (Fig. 4).
147 In the literature, the term “African Surface” generally has a genetic implication.
148 The African Surface was originally defined by L.C. King as a flat planation surface of
149 continental extent that had been leveled down to sea level until the Early Tertiary (King,
150 1948; 1967). In King’s paradigm, escarpment retreat from the coasts towards deep
151 continental interiors as a result of pedimentation was the shaping agent of a flat African
152 continent. Later work showed that the African Surface could have a significant original
153 topography and relief and even comprised the Great Escarpment of Southern Africa
154 (e.g., Partridge and Maud, 1987). For Burke and Gunnell (2008), the topography and

155 the main escarpments of the continent result from the uplift and incision of the African
156 Surface as a consequence of the growth of the plate-scale basin-and-swell relief (Fig. 1).
157 Such a model implies a low-lying and flat continent and therefore a low-lying and flat
158 African Surface before 30 Ma i.e., at the time mantle dynamics is inferred to have
159 started imprinting the continent's topography.

160 In this work, we argue that West African bauxitic remnant landscapes do not
161 define a planation surface as defined by King. Instead of pedimentation, weathering
162 enhanced by efficient drainage of the lateritic regolith that was maintained by slow river
163 incision to produce a hilly bauxite-capped landscape of moderate local relief (<100 m)
164 and wavelength (5-20 km) (Chardon et al., 2006; Fig 3). As a smooth but differentiated
165 landscape efficiently drained by a river network (Grandin, 1976; Chardon et al., 2006),
166 the African Surface had a significant long-wavelength (≥100 km) topography, relief and
167 slopes and could not have been flat at sea level elevation except along coasts. This is
168 further documented by the present study (see below) and shows that the African surface
169 cannot be used as a simple flat elevation datum for measuring surface uplift.

170 Outside the Cenozoic sedimentary basins, stepwise dissection of the African
171 Surface produced mosaic landscapes made of successive remnants of lateritic landforms
172 with specific geomorphic, sedimentological and petrological characteristics (Michel,
173 1959, 1973; Boulet, 1970; Eschenbrenner and Grandin, 1970; Boulangé et al., 1973;
174 Grandin, 1976; Gunnell, 2003; Burke and Gunnell, 2008; recent reviews by Beauvais
175 and Chardon, 2013; Grimaud et al., 2014, 2015). The Intermediate Surface designates a
176 landscape whose remnants are preserved below bauxitic relicts of the African Surface
177 and above younger lateritic pediments (Fig. 3). Relicts of the Intermediate Surface bear
178 ≥ 40 m-thick weathering profiles topped by a ferricrete that is easily distinguishable
179 from the bauxites of the African surface or the pediments. Outside Cenozoic

sedimentary basins, Intermediate Surface relicts typically delineate wide river valleys between bauxitic relief remnants forming interfluves (Fig. 3). The Intermediate Surface therefore comprises residual reliefs inherited from the Bauxitic African Surface; it has a differentiated topography and local relief and - like the African Surface - may not be considered as an originally flat regional topographic marker.

The end of bauxitic weathering coincides with the onset of the dissection of the African Surface. Similarly, the weathering and ultimate development of the Intermediate ferricrete ended with incision of the Intermediate Surface (Beauvais and Chardon, 2013). These paleolandscape abandonment ages are constrained by Ar-Ar age groups of K-Mn oxides sampled in the weathering profile of each relict surface at the Tambao type locality in Burkina Faso (Beauvais et al., 2008; Fig. 2). A 55-45 Ma age group confirms the Early- to Mid-Eocene age of the late bauxitic landscape and its abandonment around 45 Ma, whereas a 29-24 Ma age group constrains the Latest Oligocene abandonment age of the Intermediate landscape (Beauvais and Chardon, 2013).

Given their type geomorphology and regolith and the wide distribution of their relicts over the sub region (Beauvais and Chardon, 2013; Grimaud et al., 2014), the African Surface (referred to as S1) and the Intermediate Surface (S2) are decisive paleolandscape datum that are used here to investigate the regional relief and drainage configuration before their respective abandonments. Our study primarily relies on field surveys allowing assessing the spatial relationships between S1 and S2 remnants, Cenozoic sediments and the modern drainage network and alluviums over key areas of the sub region (Figs. 4 to 6). Given the dense spatial distribution of S1 and S2 landscape remnants, we also constructed the geometry of S1 and S2 surfaces at the scale of the sub region in order to extract their large-scale drainage networks.

205

206 **4. Regional topographies and drainages reconstruction protocol**

207 4. 1. Construction of S1 and S2 present-day geometry

208 To reconstruct S1 and S2 surfaces geometries, we built an irregular triangulated
209 mesh using the DSI method designed for full 3D representation of complex geological
210 objects (Mallet, 1992; Figs. 7a and 7d). Spatially varying resolution is a motivation for
211 using triangulated surfaces as compared to 2D grids, because they allow low surface
212 nodes densities (larger triangles) in smoothly varying areas and higher densities (smaller
213 triangles) in high curvature areas. Additionally, a range of constraints is used to ensure
214 geometrical consistency of the surfaces (e.g., no self-intersections), as well as
215 consistency between surfaces (e.g., no intersection). In practice, DSI solves for the
216 optimal location of the surface nodes to minimize a weighted sum of the surface
217 roughness and constrain misfit (Mallet, 1997, 2002; Caumon et al., 2009). Strict
218 constraints restrict the degree of freedom of surface nodes: a node ascribed to a surface
219 remnant data point is frozen to a given location in space. In addition to this data-points
220 compliance, soft constraints are honored in a least-squares sense: nodes are forced to lie
221 above the present day topography as well as above or below the other triangulated
222 surface (S1 above S2 above topography). This procedure allows ensuring the
223 hydrological consistency of the surfaces and accounting for the composite nature of the
224 S2 Intermediate landscape that comprises residual S1 reliefs (see Supporting
225 Information). Finally, the progressive increase in triangulated surface resolution during
226 construction, from an initial state based solely on S1 and S2 remnant data-points, allows
227 for both the data compliance and geometrical consistencies to be preserved in domains
228 where nodes are created (triangles are subdivided) beyond the initial resolution of the
229 surface remnant data sets. We verified the robustness and sensitivity of our workflow

using a synthetic case calibrated to the dimensions of typical West African surfaces' topography and relief (see Supporting Information).

4. 2. Denudation of S1 and S2

Reconstructed S1 and S2 surface geometries represent the present-day geometry of past regional topographies that have potentially undergone lithospheric deformation after their abandonment (Figs. 7a and 7d). Among the sources of deformation, the easiest one to account for is the flexural response of the lithosphere to erosion and sedimentation since their abandonment. We therefore corrected S1 and S2 triangulated surfaces from the flexural isostatic deformation of the lithosphere due to denudation and sediment deposition that distorted their geometry since their abandonment (see West et al., 2013 for a comparable approach).

At the locations of paleolandscape remnants, by definition, no denudation occurred since their abandonment. Those paleolandscape remnants constitute densely distributed summits of the region whose envelope, compared to the present day topography, constrains the amount of incision since surfaces abandonments (e.g., Fig. 3). Flexural isostasy wavelength of the old (~2 Ga) and cold West African lithosphere is expected to be much longer (several hundreds of km) than the typical horizontal distance between paleolandscape remnants (i.e., a few tens of km; Figs. 7a and 7d). The characteristic wavelength of incision of S1 and S2 is thus small enough to assume that the local relief, and therefore the denudation produced by incision, is not affected by flexural isostatic deformation. Hence, we computed denudation maps of S1 and S2 by subtracting the present-day topography from their surface geometries (Figs. 8a and 8c).

4. 3. Flexural isostatic correction of surfaces geometries

We computed the change in crustal thickness due to post-S1 and post-S2 erosion and sedimentation and the resulting flexural isostatic response (Figs. 8b and 8d). To do this, we used the formulation of Braun et al. (2013) that calculates the deflection of a thin elastic plate assuming the effective elastic thickness (EET) is linked at depth to a given isotherm. We used a 128x128 grid, 2600x1900 km in size. We assumed a 36 km thick crust with a density of 2800 $kg.m^{-3}$, a 150 km thick lithosphere with a mantle density of 3300 $kg.m^{-3}$ and a basal temperature of 1300°C. We have tested effective elastic thicknesses ranging from 30 to 50 km (isotherms 250° to 450°). For a 50 km EET, isostatic uplift ranges from 0 to 600 m for S2 and -200 to 800 m for S1 (Figs. 8b and 8d). For lower values of EET, uplift amplitudes are higher (up to 650 m for S2, -300 to 1000 m for S1) with identical map patterns. A simple Airy isostatic compensation calculation using the same grid leads to the same regional uplift pattern as that produced with a 50 km EET, but with a noise at the cell scale that is not realistic with regard to a flexural isostasy wavelength. We therefore chose to use the 50 km EET for correcting S1 and S2 surfaces geometries from denudational flexural isostasy (Figs. 8b and 8d).

Maps of Figures 8b and 8d represent rock uplift i.e., the displacement of rocks with respect to the geoid (England and Molnar, 1990), whereas it is surface uplift - defined as the denudation subtracted from rock uplift - that should be used for correcting S1 and S2 surface geometries. But those surface geometries are constrained by S1 and S2 paleolandscape remnants, which have undergone no denudation since their abandonment. Accordingly, rock uplift was used directly for correcting S1 and S2 (Figs. 7b and 7e). Corrections generally tend to reduce the large-scale topographic amplitude of surface geometries without modifying their first-order relief map pattern (Figs. 7a and 7b; 7d and 7e). Drainages were then extracted from the corrected surface

geometries (Figs. 7c and 7f; see Supporting Information). These drainages (Figs. 7c and 7f) are consistent with higher-resolution field investigations made over key areas (Figs. 4 to 6), validating the construction and isostatic correction procedures. The resulting Late Oligocene (S2) and Mid-Eocene (S1) regional physiographic stages are then interpreted from paleogeographic maps (Fig. 9), which combine the extracted drainages and the onshore paleoenvironmental sedimentary record compiled from various sources (Faure, 1966; Greigert, 1966; Greigert and Pougnet, 1967; Monciardini, 1966; Charpy and Nahon, 1978; Lang et al., 1986; Conrad and Lappartient, 1987; Reijers, 2011 and the present work).

5. Geomorphic configuration along key portions of the drainage

5. 1. Iullemmeden basin

Differential elevation of S1 and S2 tends to decrease from the exposed West African Paleoproterozoic basement towards the southern margin of the Iullemmeden basin (Colin et al., 2005; Beauvais et al., 2008; Figs. 2 and 4). There, fluvial sediments of the Continental Terminal overly S1 bauxitic weathering profiles developed upon Pre-Cenozoic bedrocks (Greigert, 1966; Gavaud, 1977, Beaudet et al., 1977b; our own field observations). The Continental Terminal also tops Mid-Eocene marine series in the rest of the basin and a temporal and spatial correlation is established between the S1 surface and those series (Fig. 4). Instead of dipping under the basin infill, S2 is preserved as conspicuous mesas capping the Continental Terminal and its adjoining basement (Dresch and Rougerie, 1960; Faure, 1966; Greigert, 1966; Gavaud, 1977; Beaudet et al., 1977b; Kogbe, 1978; our own field observations; Fig. 4). Chronostratigraphic constraints on the Continental Terminal are Oligocene mammals, fishes and woods (Radier, 1953, 1959) as well as Mid-Eocene to Oligocene pollens (Lang et al., 1990).

Weathering and duricrusting of S2 at 29-24 Ma as constrained by Ar-Ar geochronology of K-Mn oxides in Tambao (Beauvais et al., 2008; Fig. 4) are consistent with biostratigraphy and allow restraining the age of the Continental Terminal from Lutetian to Rupelian (49-29 Ma).

S2 plateaus define a very smooth regional surface (Fig. 4), which has been dissected by the Niger River and its tributaries (Fig. 5a). Incision of S2 led to the exposure of its weathering profile developed on sandstones and argillites of the Continental Terminal (Réformatsky, 1935; Gavaud, 1977; our own field observations; Fig. 5a). The dense spatial distribution and large size (up to tens of km) of S2 plateaus as well as their clear-cut photointerpretation signature validated by field control prompted us to reconstruct the geometry of S2, which displays two main features (Fig. 5b). The most prominent one is a ca. 200 km wide, NW trending asymmetrical trough with a short southwestern flank steeper than its northeastern flank and a hinge line roughly coinciding with the present day course of the Niger River. The second feature is a N-S trending valley roughly coinciding with the trace of the Dallol Bosso that widens towards its junction with the NW trending trough (Fig. 5b). We interpret this topographic pattern to reflect the main drainage axes of the region before abandonment of the S2 landscape in the Late Oligocene. The map shows that those drainage axes were already the Niger and the Dallol Bosso at their current location at the time. This interpretation is reinforced by the fact that the S2 ferricrete cements alluvial gravels or sand blankets (even where atop weathered argillites) on plateaus adjoining those modern rivers, forming the alluvial terraces along those paleo-river courses (see also Greigert, 1966; Beaudet et al., 1977b). The map also suggests that the present-day Sokoto and Zamtara Rivers were already tributaries of the Niger River in the Late Oligocene (Fig. 5b).

330

331 5. 2. High Niger valley and inland delta

332 In the northernmost High Niger catchment (Fig. 2), S1-S2 differential elevation
333 may attain 400 m and decreases towards the internal delta where S1 and S2 tend to
334 merge (Beauvais and Chardon, 2013; Grimaud et al., 2014). This is confirmed by field
335 observations at the northern margin of the delta, where S1 and S2 duricrusts cap a
336 laterally continuous weathering profile developed on Neoproterozoic sandstones (Fig.
337 6a). Around Ségou, both duricrusts are seen to mantle low (< 30 m-high) residual hills
338 dominating a pediplain (Fig. 6b). Comparable hills emerge from the inland delta
339 alluviums further to the northeast (data points in Fig. 6a). Given the low (< 40 m) relief
340 of the composite S1/S2 landscape, both types of duricrust may not only occupy hills but
341 are also seen in man-made pits in the pediplain (Figs. 6c and 6d). In the Niger River
342 course itself, a bauxitic weathering profile capping the Neoproterozoic sandstones even
343 crops under alluviums (Fig. 6e). Mapping of S1 and S2 duricrust remnants on the slopes
344 of the Niger valley around the delta (Fig. 6a) indicates that the composite S1-S2
345 weathering profile carpets the entire valley (Fig. 6f). Therefore, the valley likely had its
346 current cross-profile by the end of bauxitic weathering and has undergone very limited
347 relief evolution since then (Fig. 6f). In other words, the High Niger drainage axis
348 already existed by the Mid-Eocene (i.e., ~45 Ma). The stability of the valley is probably
349 structurally controlled for it occupies a syneclise in the Neoproterozoic sandstones
350 (Urvoy, 1942; Fig. 6f). The Late Oligocene S2 weathering profile capping the
351 Neoproterozoic sandstones is directly overlain by the Quaternary inland delta (Figs. 6e
352 and 6f). This precludes preservation of Pre-Quaternary Cenozoic fluvial sediments in
353 the High Niger valley as inferred by Urvoy (1942) and Erhart (1943), who mistook the
354 S1 / S2 weathering profile developed on the Precambrian sandstones for the Continental

355 Terminal (e.g., Bassot et al., 1980). The High Niger valley has therefore remained a
356 sediment bypass zone since at least the Mid-Eocene.
357
358 5. 3. Niger River elbow region
359 The Niger River elbow region in between the inland delta and the Iullemmeden
360 basin (Fig. 2) has been surveyed by Beaudet et al. (1977a, 1977b, 1981a) and Michel
361 (1977). Those authors have shown that the S2 ferricrete capping the mesas of the region
362 (i.e., the relicts of the "fundamental topography" of Beaudet et al., 1977a)
363 systematically dips towards the modern river and cement alluvial gravels in the vicinity
364 of its course, arguing for its antiquity. Fieldwork also led Beaudet et al. (1981a) to the
365 same conclusion for the Tilemsi River, a tributary of the Niger draining the western
366 flank of the Adrar des Ifoghas massif (Fig. 2). Those observations are consistent with
367 our investigation upstream and downstream the elbow region (Figs. 5 and 6). The 29-24
368 Ma minimum age of S2 argues for the stability of the Niger drainage since the Late
369 Oligocene.
370
371 5. 4. Sourou valley
372 Our field surveys reveal that the Sourou delta (Fig. 2) emplaced in a shallow
373 trough carpeted with a weathering profile developed on Neoproterozoic sandstones and
374 topped by bauxites and Intermediate ferricretes. S1 and S2 duricrusts cap hills emerging
375 from the delta alluviums and occur along the margins of the plain. S1 and S2 relicts see
376 their elevation and differential elevation increase eastward from the Sourou valley
377 (Boulet, 1970; Beauvais and Chardon, 2013), the valley being bounded to the west by
378 the Bandiagara plateau (See Figs. 2 and 6f). Our observations and interpretation are
379 consistent with the bauxite occurrences map of Petit (1994) and well logs in the delta

(Koussoubé, 2010). But the Cenozoic sediments inferred by Urvoy (1942) to underlie the delta (the "Continental Terminal" of the later authors) is precluded because the S1/S2 weathering profile was again mistaken for pre-delta sediments. Therefore, the morphosedimentary structure of the Sourou valley is indicative of a drainage axis existing since at least the Mid-Eocene (i.e., minimum age of the bauxites), which remained a sediment bypass until installation of the delta in the Quaternary.

The Sourou River extends via a wind gap into a river flowing eastward to the Low Niger (Fig. 2). As opposed to the uppermost north-flowing High Volta, a south-flowing Sourou could not have generated the delta considering the very limited size and relief of its catchment. The delta is indeed fringed to the northeast by the Niger watershed (Fig. 2), which would have remained stationary since the Late Oligocene (section 4.1; Fig 5b). Furthermore, the Sourou River still receives one-sixth of the High Volta waters and still flows northward up to 50 km north of their confluence (Palausi, 1959). We therefore interpret the connection of the Sourou to the Volta as resulting from overspill of the delta formed by the Sourou River that used to flow into the Niger. Delta formation and ultimate drainage reversal of the river must have resulted from surface uplift in the area of the current wind gap, which is also attested by efficient erosion of the S1 and S2 landscape remnants in between the Sourou and the Niger elbow (e.g., Beaudet al., 1981b).

6. Reconstitution of two Paleogene relief and drainage stages

6. 1. Late Oligocene stage (S2)

Corrected S2 surface geometry strikingly mimics today's topography, with the High Niger, Low Niger and Sourou valleys being clearly delineated and a drainage divide similar to the current one (Figs. 2, 7b and 7c). The drainage extraction procedure

405 imposed oceanic outlets to all drains. Some water gaps have thus been forced, such as
406 that linking the High Niger to the Senegal catchment north of Bamako (Fig. 7b). A
407 divide was also generated NW of Gao between the Low and High Niger (Fig. 7b). As
408 field evidence attests to the existence of a continuous Niger River course by the end of
409 S2 landscape stage in that area (section 4.3), a "Gao divide" may be reasonably
410 considered as irrelevant given the resolution of the method. As a way of consequence,
411 the water gap connecting the High Niger to the Senegal drainage is precluded because
412 the Niger could not overspill into the Senegal drainage and, at the same time, flow
413 across the Gao sill to form a major river valley across the Iullemmeden basin (Fig. 5b).
414 Extracted drainage displays a Sourou River flowing south into a Volta drain (Fig.
415 7b). However, this connection occurred only in the Quaternary (section 4.4). Therefore,
416 the divide generated between the Sourou and the Niger valleys near Gao (Fig. 7b) may
417 be ignored in the interpretation (Fig. 7c). Nonetheless, this divide must somehow reflect
418 uplift-driven formation of the current wind gap isolating the Sourou River from the
419 Niger (Fig. 2) and later drainage reversal of the Sourou River (see below). One must
420 therefore consider a Sourou River already flowing northeastward into the Low Niger in
421 the Late Oligocene (Fig. 7c).
422
423 6. 2. Mid-Eocene stage (S1)
424 Corrected S1 surface geometry displays a marginal upwarp forming the
425 continental divide with a steep seaward slope and a gentle northward slope, which
426 includes large valleys plunging NE i.e., the High Niger, the Sourou, and a Paleo-Volta
427 (Figs. 7e and 7f). A modern-like Senegambia catchment comparable to that of the Late
428 Oligocene stage (Fig. 7c) is also marked (Fig. 7f), as attested by extensive mapping of
429 S1 and S2 by Michel (1959, 1973). A divide isolates the Sourou from the Niger valley

and a water gap connects the Sourou valley to an upper drain of the Paleo-Volta drainage (Fig. 7e). This configuration is comparable to the drainage extracted from S2 geometry (Fig. 7b). Both this divide and water gap may therefore be precluded for the same reasons as those invoked in the S2 case, especially considering the fact that the southern coastline of the Tethys was located SW of Gao in the Mid-Eocene (i.e., at the time S1 was being ultimately weathered and duricrusted; Fig. 7f). Hence, the Sourou River must have flown directly to the sea near Gao by the Mid-Eocene (Fig. 7f). The water gap allowing the lower High Niger to flow into the Senegal drainage would imply a loop in the river very near to the seashore, allowing back flow across the marginal upwarp. Such a configuration is unlikely given the very low relief and slope of S1 and the lack of evidence for paleo-river course remnants in that area (Beaudet et al., 1977a). One must therefore consider that a Mid-Eocene High Niger used to flow northeastward to the sea (Fig. 7f).

7. Interpretation

7. 1. Oligocene paleogeography: antiquity of the West African drainage

The modern Niger drainage was established by the Late Oligocene and already comprised the High Niger and its tributaries draining the Hoggar swell (Fig. 9a). The uppermost High Niger watershed was probably located at the southernmost limit of its uncertainty domain shown in Fig. 7c given the reconstituted S2 longitudinal profiles of the High Niger and short coastal River drains, all pointing to a continental divide near its current location (Grimaud et al., 2014). The Senegambia catchment had also already acquired its current shape and its main drains (Fig. 7c). The fact that S2 paleolandscape remnants systematically dip towards the main present day river courses of the region (Grimaud et al., 2014) and the similarity between the drainage extracted from S2

455 corrected geometry and that of the current drainage (Figs. 9a and 9b) further attest to the
456 stability of the main drains since the Late Oligocene. Connection of the Sourou River to
457 the Volta and limited headward migration of the uppermost Niger watershed would be
458 the only adjustments of the drainage since the Late Oligocene (Figs. 9a and 9b).
459
460 7. 2. Mid-Eocene paleogeography
461 In the Mid-Eocene, the drainage of West Africa was organized on both slopes of
462 a marginal upwarp isolating a marine intracratonic basin connected to the Tethys
463 (Guiraud et al., 2005) from the Central and Equatorial Atlantic Ocean (Figs. 9c). Short
464 rivers drained the seaward slope of the marginal upwarp, whereas longer drains, such as
465 the High Niger, the Sourou and a Paleo-Volta flowed northward (Fig. 9c). The alluvial
466 facies of the nascent Niger delta suggests that a (short) seaward-flowing Benue drain
467 fed the delta (Fig. 9c). As both slopes of the marginal upwarp are carved by major
468 valleys at a high angle to its trend, any river crossing its crest would inevitably connect
469 both seas, forming seaways that are not substantiated by the geological record. This,
470 together with the fact that S1 bauxites and marine Paleogene sediments are mutually
471 exclusive (Millot, 1970), argues for a continental divide coinciding with the crestal
472 region of the marginal upwarp in the Mid-Eocene (Figs. 9c). The uncertainty on that
473 divide for the uppermost High Niger (Figs. 7f and 9c) may be reasonably restrained
474 towards its southwestern limit as suggested by the geometry of S1 along paleo-long
475 profiles of both the High Niger and short coastal rivers (Grimaud et al., 2014).
476
477 7. 3. Establishment of the modern drainage
478 Connection of the Niger catchment to the Equatorial Atlantic Ocean is at least
479 29 Ma old i.e., the age of the oldest preserved weathering of the S2 landscape that

480 fossilizes the current river courses (e.g., Fig. 5). Actually, acquisition of the modern
481 drainage configuration most probably dates back to 34 Ma assuming it triggered
482 building of the coastal Niger delta at the Eocene - Oligocene boundary (biostratigraphic
483 age in Doust and Omatsola, 1990). The Niger catchment has indeed remained the
484 delta's most prominent supplier. Despite episodic overspill into the Benue's catchment
485 during the recent Quaternary, the Chad basin (Figs. 1 and 2) remained an active sag
486 basin trapping sediments throughout the Cenozoic (Burke, 1976; Talbot, 1980).
487 Furthermore, the Benue drainage appears to have remained isolated from the Congo
488 basin (Fig. 1) by the Cameroon volcanic Line (e.g., Ségalen, 1967; Fritsch, 1978; Fig.
489 2) since the Eocene. Therefore, the Benue River catchment must have kept its current
490 limited size throughout the Cenozoic and could not contribute significantly to the Niger
491 delta compared to the Niger River.
492 Modification of the regional physiography between the Mid-Eocene (~45 Ma)
493 and the Late Early Oligocene (~29 Ma) resulted in a major inland shift of the
494 continental divide, east of the Guinean Rise, of up to 1000 km and required
495 entrenchment of the marginal upwarp to allow opening of at least two major drainage
496 basins (Niger and Volta) on the Equatorial Atlantic Ocean (Figs. 9a, 9c and 10).
497 Emplacement of alluvial systems of the Continental Terminal followed post-Ypresian
498 (~48 Ma) sea retreat (Figs. 10a and 10b). The absence of evaporites in the
499 Iullemmenden fan (excluding the hypothesis of a playa-bearing closed depression),
500 paleo-current directions in the fan (our own field data), and map configuration in Fig.
501 5b suggest that the course of the Niger River was established during building of the fan.
502 Aggradation-driven overspill of the Iullemmeden Fan is therefore a plausible
503 mechanism for connecting the Niger to a Benue drain. Nevertheless, a capture by
504 headward erosion of a Benue tributary may not be ruled out, but would have had to

505 occur before Iullemmeden fan installation. Rearrangement of the Volta drainage
506 involved establishment of a water gap across the marginal upwarp as well as drainage
507 reversal, implying seaward tilt of the catchment (Figs. 9 and 10). Several lines of
508 evidence reported below suggest that such a tilt may have resulted in the formation of
509 an internal delta against the ancient divide before connection of the Volta into the
510 seaward drainage. This sill coincides with one of the highest knickzones in West Africa
511 (KZ; Fig. 2) that exists since at least 11 Ma (Grimaud et al., 2014). This knickzone also
512 currently acts as the spillway for the vast plain occupying the Paleozoic Volta basin (Fig.
513 2) and where airborne magnetic data allowed imaging a major meandering paleochannel
514 transecting the main current drains (Jessell et al., 2015). Such a paleochannel suggests
515 the existence of a transient flood plain formed at the time of drainage reversal before
516 overspill into the Atlantic drainage.
517 Late Oligocene paleogeographic reconstruction (~29-24 Ma; Fig. 9a) post-dates
518 the emplacement of large alluvial systems of the Continental Terminal (i.e., megafans),
519 which had undergone deformation and erosion after settling of the S2 ferricrete (Figs.
520 10a and 10b). In the eastern part of the study area, this deformation is documented by (i)
521 the occurrence of Oligocene fluvial sediments equivalent to the Continental Terminal at
522 the top of the Atakor range in the Hoggar swell above 2500 m elevation (Rognon et al.,
523 1983; Figs. 2 and 11), (ii) erosion of the Continental Terminal at the northern margin of
524 the Iullemmeden basin and (iii) the geometry of the basin indicative of warping and
525 southward migration of depocenter on the propagating piedmont of the swell (Fig. 11).
526 Such deformation and denudation patterns sign the amplification and propagation of an
527 epeirogenic wave (Faure, 1971), which is still active as attested by anomalies in river
528 profiles showing southwestward growth of the swell (Grimaud et al., 2014; Fig. 9b).
529 Swell growth is interpreted to have produced reversal of the Volta drainage and later

530 slope decrease of the High Niger and Sourou rivers that triggered the formation of their
531 internal deltas (Grimaud et al., 2014) (Fig. 10). The short Sourou River could not keep
532 pace with this deformation and underwent flow reversal and overspill into the Volta,
533 whereas the High Niger had a higher stream power thanks to a larger catchment
534 draining highlands under intense precipitations and was able to maintain its course.
535 Practically, epeirogenic wave propagation due to the growth of the Hoggar swell
536 explains the artificial "Gao divides" and "captures" of the High Niger by the Senegal
537 and the Sourou by the Volta on S1 and S2 corrected geometries (Figs. 7b and 7e) that
538 have recorded this deformation.
539 To summarize, sea retreat from Northwestern Africa starting in the Mid-Eocene,
540 Continental Terminal fan emplacement and their warping and incision, drainage
541 reversal of the Volta valley and the development of internal deltas are successive
542 consequences of the Hoggar hot spot swell growth (Fig. 10).
543
544 **8. Discussion**
545 The present work shows that the drainage map pattern of West Africa remained
546 essentially stationary since the Late Early Oligocene (29 Ma) and most probably the
547 Earliest Oligocene (~ 34 Ma). Antiquity of the drainage argues against the view that
548 typically stepped longitudinal profiles and elbow map patterns of African rivers are
549 Quaternary features of aggressive coastal drains having captured intracratonic basins by
550 headward erosion (Goudie, 2005). Very long term drainage stability also questions earth
551 surface process models arguing for dynamically and therefore "permanently"
552 reorganizing drainage networks in cratonic and passive margin settings (Willett et al.,
553 2014). Finally, the West African example shows that classically invoked features such

554 as abrupt elbows and/or knick points in river courses may not necessarily be diagnostic
555 of drainage capture by river piracy due to headward erosion (Bishop, 1995).
556 Mid-Eocene (~ 45 Ma) paleogeography of West Africa suggests that the
557 installation and stabilization of the current drainage between 34 and 24 Ma followed
558 regional-scale drainage rearrangement. The mechanism(s) responsible for this
559 rearrangement may not all be unequivocally identified. Nonetheless, long-wavelength
560 lithospheric deformation related to the growth of the Hoggar swell has been
561 instrumental in enhancing modification in regional slope(s) that contributed to that
562 rearrangement. Therefore, river piracy via headward erosion may not be required to
563 achieve the documented drainage rearrangement. The present work attests to the
564 permanency of long portions of river valleys since the Early Paleogene (High Niger,
565 Sourou, Volta) although some may have undergone flow reversal. Such longevity is
566 explained by the fact that these valleys are structurally controlled, as early pointed out
567 by Urvoy (1942) and Palausi (1959).
568 The stability of West African drainage map patterns warrants investigation of
569 river long profiles evolution over geological time scales (Grimaud et al., 2014). But
570 uplift histories retrieved from river profiles inversion (Paul et al., 2014) would not be
571 valid as extrapolated back in time beyond the Late or Early Oligocene (30-34 Ma),
572 which corresponds to the time of regional drainage rearrangement. Besides, river
573 inversion procedures are based on stream power law incision models that explicitly rely
574 on headward migration of knickzones, which have been shown to be stationary along
575 West African rivers during the Neogene (Grimaud et al., 2014). Moreover, the growth
576 of several hot-spot swells over Northern and Eastern Africa from the Mid-Eocene
577 onward (Burke, 1996) is likely to have triggered drainage reorganizations comparable to
578 that documented here around the Hoggar. Therefore, the main rivers draining those

579 swells must have composite profiles whose inversion in terms of uplift may be
580 challenged.

581 Drainage stabilization since the Early Oligocene sets a new framework for
582 understanding the West African craton-margin source-to-sink system. Indeed, large
583 catchments such as the Niger, the Volta and Senegambia have kept a constant geometry
584 since 29-34 Ma. The Niger catchment has been the Niger delta's most prominent
585 supplier since that time. Therefore, increasing Neogene clastic sedimentary flux to the
586 delta that has attained a peak in the Pliocene (Robin et al., 2011) has responded to the
587 growth of the Hoggar swell and potentially to climatically driven change in erosion
588 efficiency, but not to drainage reorganization. Accordingly, the Latest Pliocene drop in
589 clastic fluxes to the delta (Jermannaud et al., 2010; Robin et al., 2011) may solely be
590 due to aridification that dried out the Niger's tributaries draining the Hoggar swell (e.g.,
591 Fig. 2). Finally, stability of the Senegambia catchment offers the opportunity to
592 investigate relationships between the sedimentary record of the Senegal basin and the
593 denudation history of the catchment since the Mid-Eocene (i.e., age of the S1 bauxites;
594 Fig. 10). By contrast, a major change in the sedimentary record of the Equatorial margin
595 of Africa is expected consecutively to the connection of its two most prominent
596 catchments (Niger and Volta) to the Equatorial Atlantic Ocean after an Early Paleogene
597 (pre ~34 Ma) period of subdued clastic inputs by short rivers. The main cause for this
598 stratigraphic turnover is the initiation and amplification of the Hoggar hot-spot swell.

599 Long-wavelength lithospheric deformation due to hot spot swell growth may
600 trigger large-scale drainage rearrangement as exemplified here by West Africa since the
601 Mid-Eocene (~48-40 Ma). But the West African example also shows that once the new
602 drainage configuration is set, ongoing swell growth may not necessarily lead to further
603 significant river network rearrangement. Maintenance of the drainage his allowed by a

very gentle (~0.3 ‰) regional slope from the Atakor's piedmont to the coast, which may be sustained by very-long wavelength swell growth (Fig. 11). On the upper southern slope of the swell where the S2 topography has been eroded the most (~1.5 km; Fig. 11), more than 600 m of denudational isostatic uplift is expected since the Latest Oligocene (~24 Ma) (Fig. 8b). This suggests that erosion of the growing swell contributed to at least one-third of the maximum finite uplift due to hot spot swell growth (~2 km; Fig. 11), the remaining two-third of the uplift being produced by dynamic asthenospheric support, isostatic compensation of magmatic underplating and potential plume thermal effect.

Our work argues for the stability of rivers crossing the West African marginal upwarp since the Early Oligocene but also shows that the upwarp earlier formed a continental divide. Periods of dual (northward and southward) drainage may therefore alternate with periods of through-going rivers tapping sediments from the continental interior and would plead for renewed margin upwarping even long after (~90 Ma) continental breakup. Still, our study shows that at least 1500 km wavelength, hot-spot related lithospheric deformation (Fig. 10) may be efficient in triggering seaward tilt of the continental surfaces leading to the connection of internal drainage to coastal rivers across low-elevation passive margins.

9. Conclusion

The main current pattern of the West African drainage such as the Niger and Volta river systems stabilized in the Late Early Oligocene (>29 Ma) and probably at the Eocene-Oligocene boundary (34 Ma). Antiquity of the drainage opens new perspective on linking offshore stratigraphic records to landform evolution of large catchments of known stationary geometry over the last ~34-29 Ma and even since ~45 Ma for the

Senegambia drainage. This result calls for caution in interpreting elbows and stepped longitudinal profiles of cratonic rivers as diagnostic of Quaternary drainage rearrangements due to aggressive headward erosion, and suggests that river piracy may be much less common than inferred in shield contexts. Reconstituted Mid-Eocene (~45 Ma) geography suggests that the drainage reorganized and stabilized after a period of dual drainage on both slopes of a marginal upwarp acting as a continental divide. Very long wavelength growth of the Hoggar hot spot swell since the Late Eocene caused regional drainage rearrangement that led to the modern physiography of West Africa. Importantly, a major regional stratigraphic turnover is expected along the Equatorial margin of Africa consecutive to the opening of at least two major catchments (Niger and Volta) on the Atlantic Ocean following a period of subdued clastic sedimentary fluxes provided by short rivers.

Acknowledgments

This work stems from extensive regional field reconnaissance and compilation work over the years, which have been supported by Toulouse University, the IRD, the TopoAfrica project (ANR-08-BLAN-572 0247-02), the CNRS and the West African eXploration Initiative (WAXI). We acknowledge current support from Total SA (TS2P project) and the gOcad research consortium. We are grateful to J. Braun for access to Flex3D that allowed for the flexural isostatic corrections. We thank G. Brocard for his review of an earlier version of the manuscript, the referees for their constructive suggestions, S. Bonnet for advise on drainage extraction and D. Huyghe for support. J.-L. Rageot, G. Besançon and Z. Garba are thanked for fruitful discussions and support during a memorable early field trip in Niger. We acknowledge AMIRA International and the industry sponsors, including AusAid and the ARC Linkage Project

LP110100667, for their support of the WAXI project (P934A) as well as the Geological Surveys / Departments of Mines in West Africa as sponsors in kind of WAXI. The data used are available upon request to the authors.

658 **References**

659 Bassot, J. P., M. M. Diallo, H. Traoré, and J. Méloux (1980), Carte géologique du
660 Mali à 1/1 500 000, *Dir. Nat. Géol. Min. Mali*.

661 Beaudet, G., R. Coque, P. Michel, and P. Rognon (1977a), Y-a t-il eu capture du
662 Niger ?, *Bull. Ass. Géogr. Franç.*, *445-446*, 215-222.

663 Beaudet, G., R. Coque, P. Michel, and P. Rognon (1977b), Altérations tropicales et
664 accumulations ferrugineuses entre la vallée du Niger et les massifs centraux
665 sahariens (Aïr et Hoggar), *Z. Geomorph. N.F.*, *21*(3), 297-322.

666 Beaudet, G., R. Coque, P. Michel, and P. Rognon (1981a), Reliefs cuirassés et
667 évolution géomorphologique des régions orientales du Mali. 1. La région du
668 Tilemsi et la Vallée du Niger de Taoussa à Gao, *Z. Geomorph. N.F.*, *38*, 38-62.

669 Beaudet, G., R. Coque, P. Michel, and P. Rognon (1981b), Reliefs cuirassés et
670 évolution géomorphologique des régions orientales du Mali. 2. Le Gourma et le
671 plateau de Bandiagara, son contact avec le Macina, *Z. Geomorph. N.F.*, *38*, 63-85.

672 Beauvais, A., and D. Chardon (2013), Modes, tempo, and spatial variability of
673 Cenozoic cratonic denudation: The West African example, *Geochem. Geophys.*
674 *Geosyst.*, *14*(5), 1590-1608.

675 Beauvais, A., G. Ruffet, O. Henocque, and F. Colin (2008), Chemical and physical
676 erosion rhythms of the West African Cenozoic morphogenesis: The (39)Ar-(40)
677 Ar dating of supergene K-Mn oxides, *J. Geophys. Res., 113*, F4007.

678 Bishop, P. (1995), Drainage rearrangement by river capture, beheading and diversion,
679 *Progr. Phys. Geogr.*, *19*, 449-473.

680 Bond, G. C. (1979), Evidence for Some Uplifts of Large Magnitude in Continental
681 Platforms, *Tectonophysics*, *61*(1-3), 285-305.

682 Boulangé, B., and G. Millot (1988), La distribution des bauxites sur le craton ouest-
683 africain, *Sci. Géol. Bull.*, *41*, 113-123.
684 Boulangé, B., J. B. Sigolo, and J. Delvigne (1973), Descriptions morphoscopiques,
685 géochimiques et minéralogiques des faciès cuirassés des principaux niveaux
686 géomorphologiques de Côte d'Ivoire, *Cah. ORSTOM Sér. Géol.*, *5*, 59-81.
687 Boulet, R. (1970), La géomorphologie et les principaux types de sols en Haute-Volta
688 septentrionale, *Cah. ORSTOM Sér. Pédol.*, *8*, 245-271.
689 Burke, K. (1976), Chad Basin - Active Intra-Continental Basin, *Tectonophysics*,
690 *36*(1-3), 197-206.
691 Burke, K. (1996), The African Plate, *S. Afr. J. Geol.*, *99*(4), 341-409.
692 Burke, K., and Y. Gunnell (2008), The African erosion surface: A continental scale
693 synthesis of geomorphology, tectonics, and environmental change over the past
694 180 million years, *Geol. Soc. Am. Mem.*, *201*, 1-66.
695 Burke, K., D. S. Macgregor, and N. R. Cameron (2003), Africa's petroleum systems:
696 four tectonic 'aces' in the past 600 million years, *Spec. Publ. Geol. Soc.*, *207*, 21-
697 60.
698 Caumon, G., P. Collon-Drouaillet, C. Le Carlier de Veslud, S. Viseur, and J. Sausse
699 (2009), Surface-based 3D modeling of geological structures, *Math. Geosci.*, *41*,
700 927-945.
701 Chardon, D., V. Chevillotte, A. Beauvais, G. Grandin, and B. Boulangé (2006),
702 Planation, bauxites and epeirogeny: One or two paleosurfaces on the West
703 African margin?, *Geomorphology*, *82*(3-4), 273-282.
704 Charpy, N., and D. Nahon (1978), Contribution à l'étude lithostratigraphique et
705 chronostratigraphique du Tertiaire du bassin de Côte d'Ivoire, *Dept. Sci. Terre Sér.*
706 *Doc. Univ. Abidjan 18*, 1-40.

707 Chudeau, R. (1909), *Missions au Sahara - Tome II. Sahara Soudanais*, 326 pp.,
708 Armand Colin, Paris.
709 Chudeau, R. (1919), La capture du Niger par le Taffassasset, *Ann. Géogr.*, *28*(151),
710 52-60.
711 Colin, F., A. Beauvais, G. Ruffet, and O. Henocque (2005), First Ar-40/Ar-39
712 geochronology of lateritic manganiferous pisolites: Implications for the
713 Palaeogene history of a West African landscape, *Earth Planet. Sci. Lett.*, *238*(1-2),
714 172-188.
715 Conrad, G., and J. R. Lappartient (1987), The Continental-Terminal, Its Role in the
716 Geodynamic Evolution of the Senegal-Mauritania Basin during the Cenozoic, *J.*
717 *Afr. Earth Sci.*, *6*(1), 45-60.
718 Doust, H., and E. Omatsola (1990), Niger delta, *Am. Ass. Petrol. Geol. Mem.*, *48*,
719 201-238.
720 Dresch, J., and G. Rougerie (1960), Observations morphologiques dans le Sahel du
721 Niger, *Rev. Géomorph. Dyn.*, *11*, 49-58.
722 England, P., and P. Molnar (1990), Surface Uplift, Uplift of Rocks, and Exhumation
723 of Rocks, *Geology*, *18*(12), 1173-1177.
724 Erhart, H. (1943), Les latérites du moyen Niger et leur signification paléoclimatique,
725 *C.R. Acad. Sci. Paris*, *217*, 323-325.
726 Eschenbrenner, V., and G. Grandin (1970), La séquence de cuirasses et ses
727 différentiations entre Agnibiléfrou et Diébougou (Haute-Volta), *Cah. ORSTOM*
728 *Sér. Géol.*, *2*, 205-246.
729 Faure, H. (1966), Reconnaissance géologique des formations sédimentaires post-
730 paléozoïques du Niger oriental, *Mém. Bur. Rech. Géol. Min.*, *29*, 1-630.

731 Faure, H. (1971), Relations dynamiques entre la croûte et le manteau d'après l'étude
732 de l'évolution paléogéographique des bassins sédimentaires, *C.R. Acad. Sci. Paris*,
733 *272*, 3239-3242.
734 Furon, R. (1929), L'ancien delta du Niger, *Rev. Géogr. Phys. Géol. Dyn.*, *2*, 265-274.
735 Furon, R. (1931), Notes de stratigraphie soudanaise. De l'extension des grès,
736 conglomérats ferrugineux et calcaires lacustres dans les vallées du Niger et du
737 Bani, *Bull. Soc. Geol. Fr.*, *5*, 581-588.
738 Furon, R. (1932), Introduction à la géologie du Soudan occidental, *Bull. Ag. Gén.*
739 *Colonies*, *283*, 1-73.
740 Fritsch, P. (1978), Chronologie relative des formations cuirassées et analyse
741 géographique des facteurs de cuirassement au Cameroun, *Trav. Doc. Géogr. Trop.*
742 *(CEGET)*, *33*, 114-132.
743 Gavaud, M. (1977), Les grands traits de la pédogenèse au Niger méridional, *Trav.*
744 *Doc. ORSTOM*, *76*, 1-102.
745 Gilchrist, A. R., and M. A. Summerfield (1990), Differential Denudation and
746 Flexural Isostasy in Formation of Rifted-Margin Upwarps, *Nature*, *346*, 739-742.
747 Gilchrist, A. R., H. Kooi, and C. Beaumont (1994), Post-Gondwana Geomorphic
748 Evolution of Southwestern Africa - Implications for the Controls on Landscape
749 Development from Observations and Numerical Experiments, *J. Geophys. Res-*
750 *Solid Earth*, *99*(B6), 12211-12228.
751 Goudie, A. S. (2005), The drainage of Africa since the Cretaceous, *Geomorphology*,
752 *67*, 437-456.
753 Grandin, G. (1976), Aplanissements cuirassés et enrichissement des gisements de
754 manganèse dans quelques régions d'Afrique de l'Ouest, *Mém. ORSTOM, 82*, 1-
755 276.

Greigert, J. (1966), Description des formations crétacées et tertiaires du bassin des Iullemeden (Afrique occidentale), *Publ. Dir. Min. Géol. Rep. Niger*, *2*, 1-234.

Greigert, J., and R. Pougnet (1967), Essai de description des formations géologiques de la République du Niger, *Mém. Bur. Rech. Géol. Min.*, *48*, 1-238.

Grimaud, J. L., D. Chardon, and A. Beauvais (2014), Very long-term incision dynamics of big rivers, *Earth Planet. Sci. Lett.*, *405*, 74-84.

Grimaud, J. L., D. Chardon, V. Metelka, A. Beauvais and O. Bamba (2015), Neogene cratonic erosion fluxes and landform evolution processes from regional regolith mapping (Burkina Faso, West Africa), *Geomorphology*, *241*, 315-330.

Guiraud, R., W. Bosworth, J. Thierry, and A. Delplanque (2005), Phanerozoic geological evolution of Northern and Central Africa: An overview, *J. Afr. Earth Sci.*, *43*, 83-143.

Gunnell, Y. (2003), Radiometric ages of laterites and constraints on long-term denudation rates in West Africa, *Geology*, *31*(2), 131-134.

Helm, C. (2009), Quantification des flux sédimentaires anciens à l'échelle d'un continent : le cas de l'Afrique au Méso-Cénozoïque, Ph D thesis, 386 pp, University of Rennes 1, Rennes.

Hubert, H. (1912), Sur un important phénomène de capture dans l'Afrique occidentale, *Ann. Géogr. Fr.*, *21*, 251-262.

Jermannaud, P., D. Rouby, C. Robin, T. Nalpas, F. Guillocheau, and S. Raillard (2010), Plio-Pleistocene sequence stratigraphic architecture of the eastern Niger Delta: A record of eustasy and aridification of Africa, *Mar. Pet. Geol.*, *27*(4), 810-821.

779 Jessell, M., K. Boamah, J. A. Duodu, and Y. Ley-Cooper (2015), Geophysical
780 evidence for a major palaeochannel within the Obosum Group of the Volta Basin,
781 Northern Region, Ghana, *J. Afr. Earth Sci.*, *112*, 586-596.
782 King, L. C. (1948), On the Age of the African land-surfaces, *Q. J. Geol. Soc. Lond.*,
783 *104*, 439-459.
784 King, L. C. (1967), *The morphology of the Earth*, second ed., 726 pp., Oliver and
785 Boyd, Edinburgh.
786 Kogbe, C. A. (1978), Origin and composition of the ferruginous oolites and laterites
787 of Northwestern Nigeria, *Geol. Rund.*, *67*, 662-667.
788 Koussoubé, Y. (2010), Hydrogéologie des séries sédimentaires de la dépression
789 piézometrique du Gondo (bassin du Sourou) - Burkina faso / Mali, Ph D Thesis,
790 273 pp, UPMC - Sorbone University, Paris.
791 Lang, J., C. Kogbe, K. Alidou, A. Alzouma, D. Dubois, A. Houessou, and J. Trichet
792 (1986), Le sidérolithique du Tertaire Ouest-africain et le concept de Continental
793 Terminal, *Bull. Soc. Géol. Fr.*, *8*, 605–622.
794 Lang, J., et al. (1990), The Continental Terminal in West Africa, *J. Afr. Earth Sci.*,
795 *10*(1-2), 79-99.
796 Mallet, J. L. (1992), Discrete Smooth Interpolation in Geometric Modeling, *Comput.*
797 *Aided Design*, *24*(4), 178-191.
798 Mallet, J. L. (1997), Discret modeling of natural objects, *Math. Geol.*, *29*, 199-219.
799 Mallet, J. L. (2002), *Geomodeling*, 612 pp., Oxford University Press, New York.
800

801 Michel, P. (1959), L'évolution géomorphologique des bassins du Sénégal et de la
802 Haute-Gambie, ses rapports avec la prospection minière, *Rev. Géomorph. Dyn.*,
803 *10*, 117-143.
804 Michel, P. (1973), Les bassins des fleuves Sénégal et Gambie, étude
805 géomorphologique, *Mém. ORSTOM*, *63*, 1-752.
806 Michel, P. (1977), Les modelés et dépôts du Sahara méridional et Sahel et du sud-
807 ouest africain. Essai de comparaison, *Rech. Géogr. Strasbourg*, *5*, 5-39.
808 Millot, G. (1970), *The geology of clays*, 429 pp., Springer-Verlag, Berlin.
809 Monciardini, C. (1966), La sédimentation éocène au Sénégal, *Mém. Bur. Rech. Géol.*
810 *Min.*, *43*, 1-66.
811 Palausi, G. (1959), Contribution à l'étude géologique et hydrogéologique des
812 formations primaires au Soudan et en Haute-Volta, *Bull. Serv. Géol. Prosp. Min.*,
813 *33*, 1-209.
814 Partridge, T. C., and R. R. Maud (1987), Geomorphic evolution of southern Africa
815 since the Mesozoic, *S. Afr. J. Geol.*, *90*, 179-208.
816 Paul, J. D., G. G. Roberts, and N. White (2014), The African landscape through
817 space and time, *Tectonics*, *33*(6), 898-935.
818 Petit, M. (1994), Carte géomorphologique du Burkina Faso à 1/1 000 000,
819 ORSTOM (IRD) - University of Ouagadougou, Burkina Faso, Ouagadougou.
820 Radier, H. (1953), Contribution à l'étude stratigraphique et structurale du détroit
821 soudanais, *Bull. Soc. Géol. Fr.*, *3*, 677-695.
822 Radier, H. (1959), Contribution à l'étude géologique du Soudan oriental. Deuxième
823 partie : Le bassin crétacé et tertiaire de Gao, *Bull. Serv. Géol. Prosp. Min. AOF*,
824 *26*(2), 327-556.

825 Réformatsky, N. (1935), Quelques observations sur les latérites et les roches
826 ferruginisées de l'ouest de la colonie du Niger français, *Bull. Soc. Géol. Fr.*, *37*,
827 575-589.
828 Reijers, T. J. A. (2011), Stratigraphy and sedimentology of the Niger Delta,
829 *Geologos*, *17*(3), 133-162.
830 Robin, C., F. Guillocheau, S. Jeanne, F. Porcher, and G. Calvès (2011), Cenozoic
831 siliciclastic fluxes evolution around Africa, *Geophys. Res. Abstr.*, *13*, EGU2011-
832 5659.
833 Rognon, P., Y. Gourinard, Y. Bandet, J. C. Koeniguer, and F. Delteildesneux (1983),
834 Précisions chronologiques sur l'évolution volcano-tectonique et
835 géomorphologique de l'Atakor (Hoggar): Apport des données radiométriques
836 (K/Ar) et paléobotaniques (bois fossiles), *Bull. Soc. Géol. Fr.*, *25*(6), 973-980.
837 Rouby, D., S. Bonnet, F. Guillocheau, K. Gallagher, C. Robin, F. Biancotto, O.
838 Dauteuil, and J. Braun (2009), Sediment supply to the Orange sedimentary system
839 over the last 150 My: An evaluation from sedimentation/denudation balance, *Mar.*
840 *Pet. Geol.*, *26*(6), 782-794.
841 Ségalen, P. (1967), Les sols et la géomorphologie du Cameroun, *Cah. ORSTOM, Sér.*
842 *Pédol.*, *5*, 137-187.
843 Séranne, M. (1999), Early Oligocene stratigraphic turnover on the West Africa
844 continental margin: a signature of the Tertiary greenhouse-to-icehouse transition?,
845 *Terra Nova*, *11*(4), 135-140.
846 Summerfield, M. A. (1985), Plate tectonics and landscape development on the
847 African continent, in *Tectonic geomorphology*, edited by M. Morisawa and J. T.
848 Hack, pp. 27-51, Allen & Unwin, Boston.

849 Summerfield, M. A. (1996), Tectonics, geology, and long-term landscape
850 development, in *Physical geography of Africa*, edited by W. M. Adams, A. S.
851 Goudie and A. R. Orme, pp. 1-17, Oxford University Press, Oxford.
852 Talbot, M. R. (1980), Environmental responses to climatic change in the West
853 African Sahel over the past 20 000 years, in *The Sahara and the Nile*, edited by M.
854 A. J. Williams and H. Faure, pp. 37-62, Balkema, Rotterdam.
855 Tricart, J. (1959), Géomorphologie dynamique de la moyenne vallée du Niger
856 (Soudan), *Ann. Géogr.*, *68*, 333-343.
857 Urvoy, Y. (1942), Les bassins du Niger. Etude de géographie physique et de
858 paléogéographie, *Mém. Inst. Fr. Afr. Noire*, *4*, 1-144.
859 Voute, C. (1962), Geological and morphological evolution of the Niger and Benue
860 valleys, *IVth Panafrican Congr.*, 189-207.
861 West, A. J., M. Fox, R. T. Walker, A. Carter, T. Harris, A. B. Watts, and B. Gantulga
862 (2013), Links between climate, erosion, uplift, and topography during
863 intracontinental mountain building of the Hangay Dome, Mongolia, *Geochem.*
864 *Geophys. Geosyst.*, *14*(12), 5171-5193.
865 Willett, S. D., S. W. McCoy, J. T. Perron, L. Goren, and C. Y. Chen (2014),
866 Dynamic Reorganization of River Basins, *Science, 343,* 1248765.
867

Figure captions

Figure 1. Topography, "basin-and-swell" relief, and main river systems of Africa. Cross-hatched patterns are divides delineating basins' septa. Dashed rivers are dried out. T – Taoudeni basin; Iu – Iullemmeden basin; Ch – Chad basin; Co – Congo basin.

Figure 2. Topography and drainage of West Africa showing selected geological elements. Rivers are shown in white (dashed where dried out since the Early Quaternary). A – Aïr; AI – Adrar des Ifoghas; KZ – Knickzone of the Lower Volta.

Figure 3. Stacked topographic cross-sections of the granite-greenstone terrains of the Yamoussoukro – Dimborko area (Central Ivory Coast; Fig. 2) showing the disposition of relicts of the bauxitic Surface (S1) and the ferricrete relicts of the Intermediate (S2) Surface (adapted from Grandin, 1976). The Bauxitic landscape has a low relief (< 70 m) compared to that of the Intermediate landscape (up to 350 m) that includes bauxite relicts. The sections trend mostly NW and encompass a total area ca. 100 x 70 km. Greenstone belts form the topographic massifs.

Figure 4. Regional cross section of the Cenozoic Iullemmeden basin and its basement illustrating the relationships between the S1 bauxitic and S2 Intermediate paleosurfaces and alluvial sediments of the Continental Terminal (line of section is located on Fig. 2). The section shows the spatial and temporal continuity established between the S1 bauxitic erosional surface and the Early to Mid-Paleogene marine sediments. Basin geometry is modified after Greigert (1966).

892 **Figure 5.** Relationships between the S2 Intermediate Surface and its weathering profile,
893 fluvial sediments of the Continental Terminal, and the Niger drainage in the southern
894 Iullemmeden basin (see Fig. 2 for location). (a) Illustration of a S2 Intermediate
895 landscape remnant and its underlying weathering profile developed from argillites (near
896 Filingué, Fig. 5b). The 35-m high cliff exposes, from bottom to top, a fine-grained
897 saprolite (yellowish), a mottled zone (brown), a carapace (reddish) and a ferricrete (slab
898 pavement). Top of whitish coarse saprolite locally crops out at the base of the cliff. Note
899 large S2 remnant in the background. (b) Contour map of the Intermediate landsurface
900 (S2) ferricrete processed from stations comparable to that shown in (a). Data were
901 automatically contoured and manually extrapolated in areas of low data density near the
902 northwestern and southeastern edges of the map. Note the Tambao locality where
903 weathering and abandonment ages of the S2 surface were constrained by Ar-Ar dating
904 (Beauvais et al., 2008).
905
906 **Figure 6.** Remnants of the Bauxitic Surface (S1) and ferricretes of the Intermediate
907 Surface (S2) in the Niger inland delta region. (a) Map view. Squares are our own field
908 observations and circles are from the literature (Michel, 1977; Bassot et al., 1980;
909 Beaudet et al., 1981b) and GoogleEarth surveys. (b) S1 Bauxite-capped hill with slopes
910 draped by the S2 Intermediate ferricrete (near Sansanding, 5 km east of the River; Fig.
911 6a). Hilltop (314 m) dominates the pediplain by less than 30 m (width of the view is ca.
912 3 km). (c) Pisolithic bauxite from a pit in the pediplain (same area, 3 km from the River,
913 284 m). (d) Contact between the Intermediate ferricrete and its underlying carapace
914 (quarry located 10 km upstream of Ségou, 292 m). (e) Cross-section in Sansanding (Fig.
915 6a) based on a series of boreholes (modified after Furon, 1931) showing the S1 bauxitic
916 weathering profile underlying the Niger alluviums. (f) Cross-section of the High Niger

River valley (dashed line in Fig. 6a). S1 bauxites (in red) and S2 ferricretes (in blue) having undergone relief inversion are shown. S1/S2 weathering profile's thickness takes into account the local relief and regional observations.

Figure 7. (a) Interpolated geometry of the Intermediate (S2) Surface. Data points are shown in black. (b) Drainage extraction from S2 geometry corrected for erosional isostasy. (c) Corresponding drainage interpretation. Divides are drawn in red with their uncertainty in grey. (d-f) Same maps as (a-c) for the Bauxitic (S1) Surface. Areas of marine flooding are shown in blue (after the paleogeographic synthesis of Fig. 9). Water gaps shown by red circles and wind gaps / divides shown by white circles in (b) and (e) were rejected in the interpretation in (c) and (f) on the basis of field observations or other considerations (see text for further explanation). Uncertainties on divides also take into account the density of data points used to construct the surfaces geometries.

Figure 8. Sources for the isostatic correction of the Intermediate Surface (S2) and the Bauxitic Surface (S1) from denudation and sediment accumulation since their abandonments ca. 24 and 45 Ma ago, respectively. (a) Denudation map computed from the subtraction of S2 topography to the present day topography. (b) Computed flexural rock uplift in response to that denudation considering a thin sheet model of lithosphere with an elastic thickness of 50 km. (c-d) Same maps as (a-b) for the S1 Surface. The grid represents the ~60 km-size cells used for inverting denudation into flexural uplift. The main features revealed by the denudation and uplift maps are (i) a marginal upwarp whose main present-day remnant is the Guinean rise, (ii) the Hoggar swell and, in the case of S1, (iii) the Iullemmeden basin in which the S1 surface is buried (compare with Figure 2 for locations).

Figure 9. Cenozoic paleogeographic / drainage configurations of West Africa. (a) Oligocene – Miocene boundary (~24 Ma). (b) Present day. (c) Mid-Eocene (~45 Ma). Area of active propagating uplift is drawn after Grimaud et al. (2014).

Figure 10. Sketch view of three stages in the relief / drainage evolution of West Africa and its continental margin. (a) Mid-Eocene (~45 Ma) period of maximum flooding. A continuous marginal upwarp marks the continental divide. (b) Early Oligocene (~34-29 Ma). Feeding of Continental Terminal fans on the Hoggar's piedmont; establishment of the modern Niger River Course; reversal of the Paleo-Volta drainage with development of an internal delta (inferred) and eventual connection to the Equatorial Atlantic Ocean. (c) Modern period (Quaternary). Further hot-spot swell propagation leads to warping and incision of the alluvial fans as well as slope decrease of the High Niger and Sourou rivers leading to the formation of inland deltas and eventual overspill of the Sourou into the Volta drainage.

Figure 11. Synthetic cross-section of West Africa from the Hoggar to the Ivory Coast margin (see Fig. 10 for location). Offshore part of the section is adapted from Helm (2009). Onshore erosional surfaces are prolonged in the sedimentary basins as sequence boundaries, which are considered as their time equivalent.

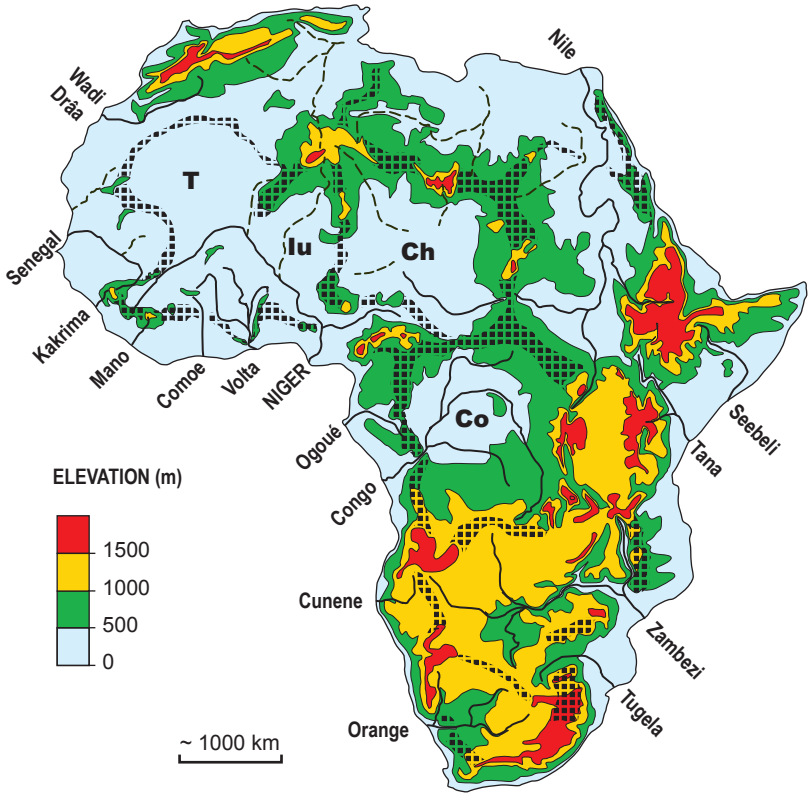

Chardon et al., Figure 1

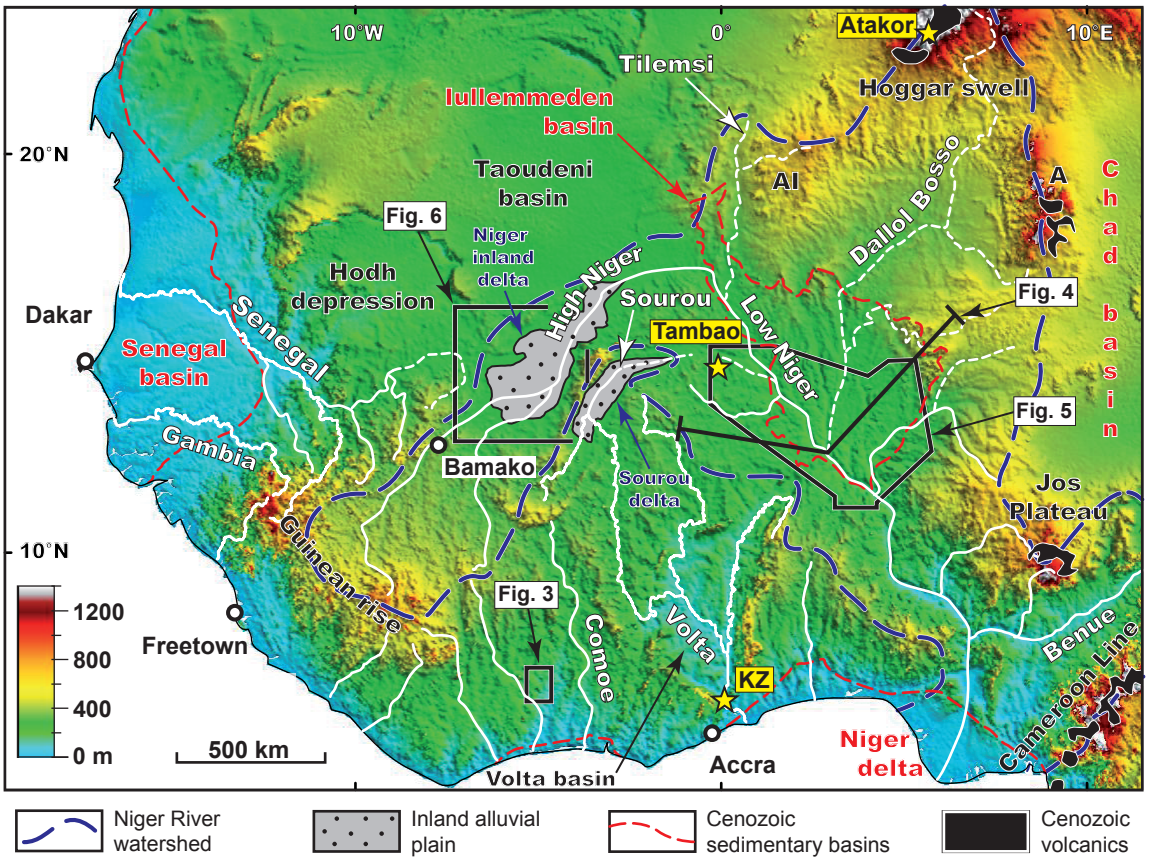

Chardon et al., Figure 2

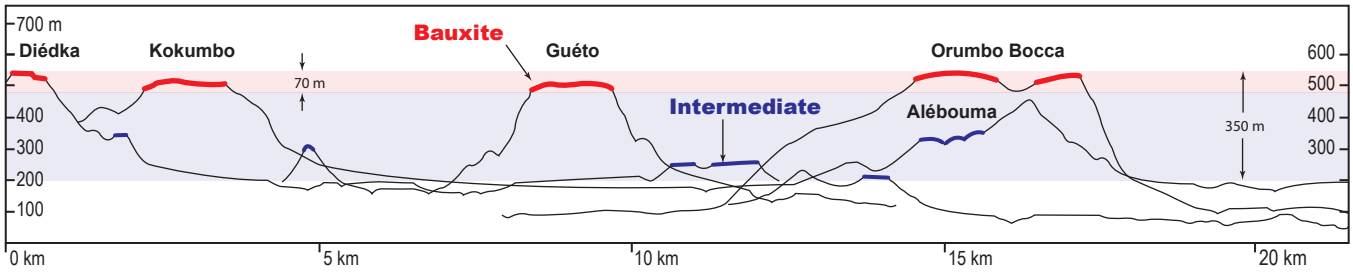

Chardon et al., Figure 3

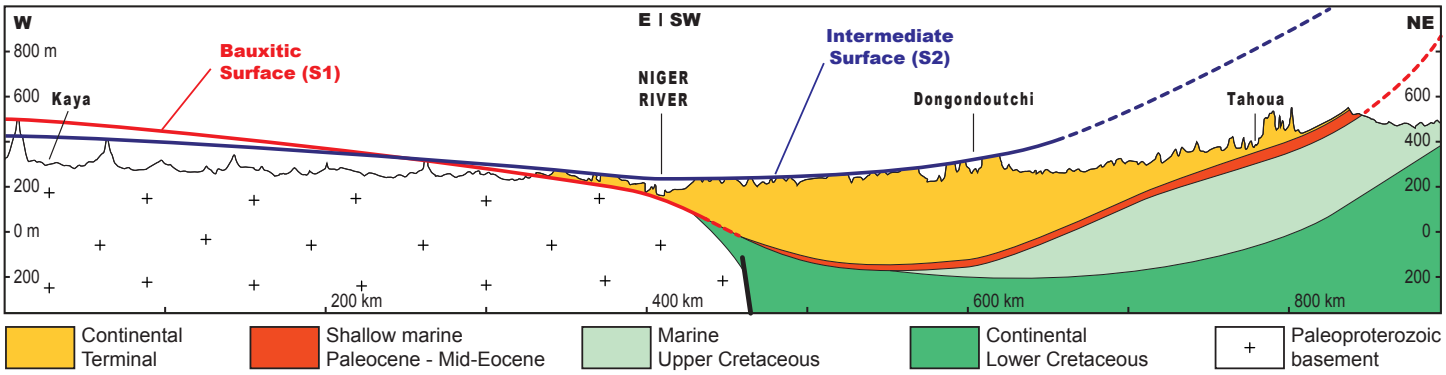

Chardon et al., Fig. 4

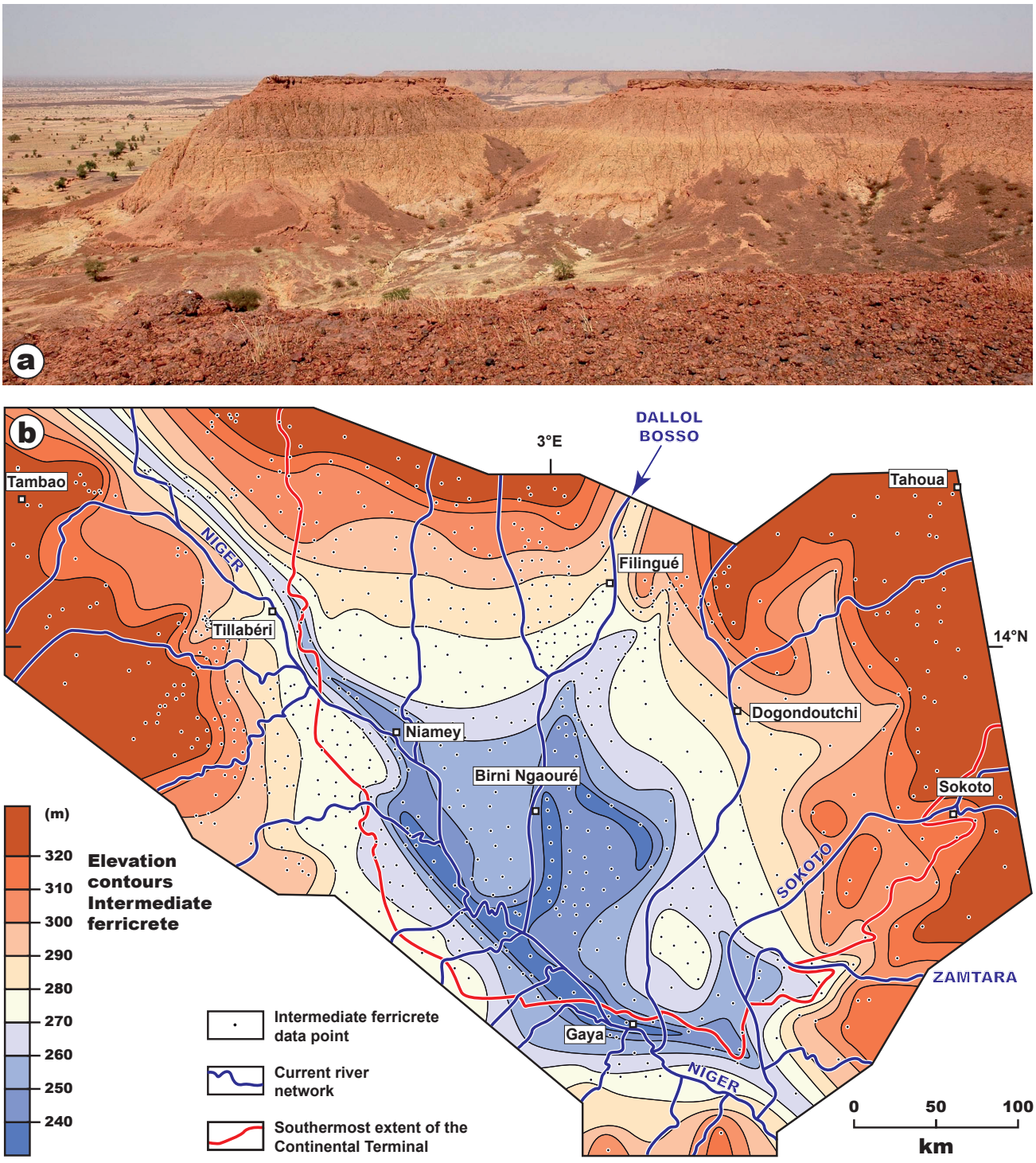

Chardon et al., Figure 5

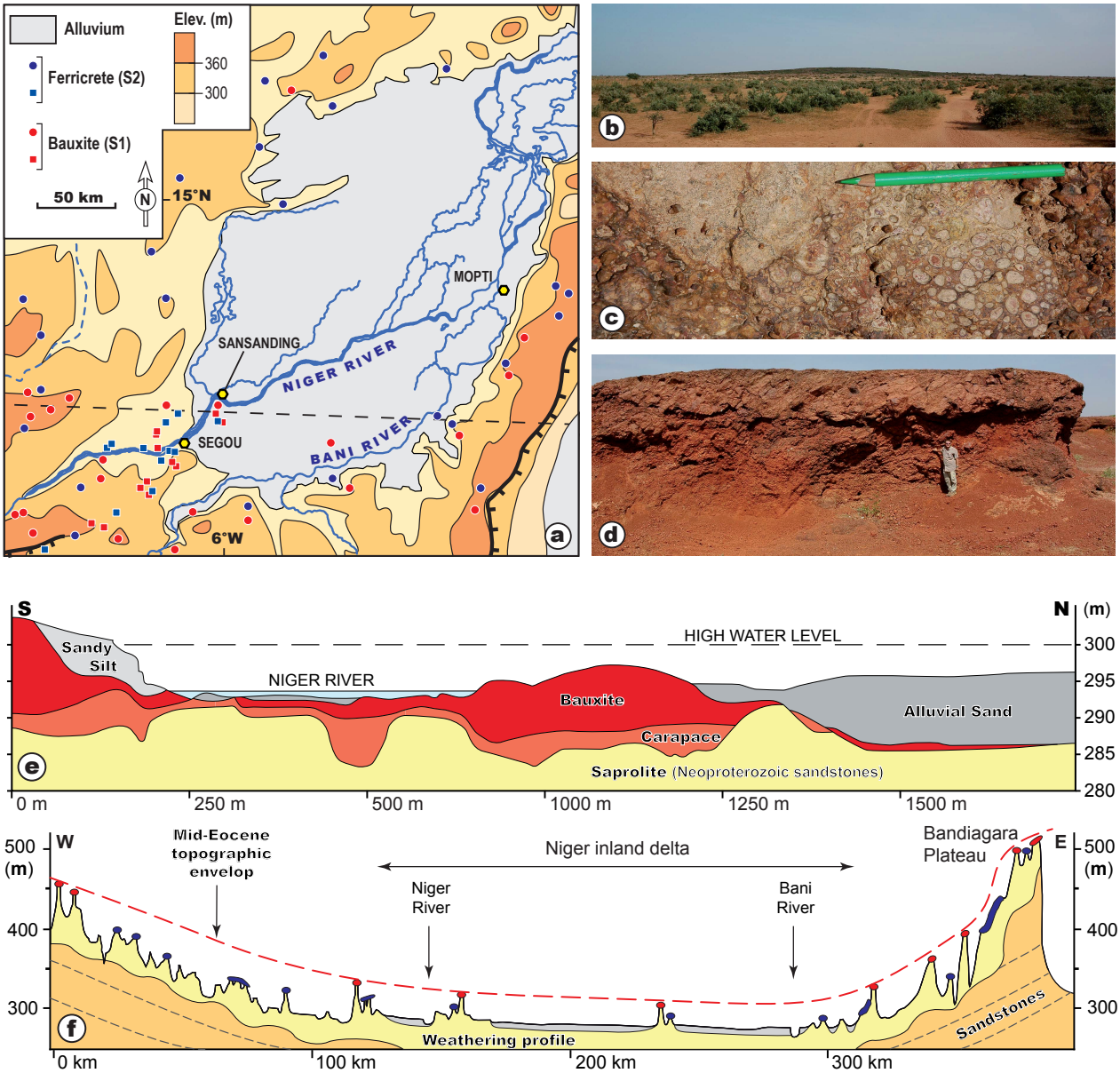

Chardon et al., Figure 6

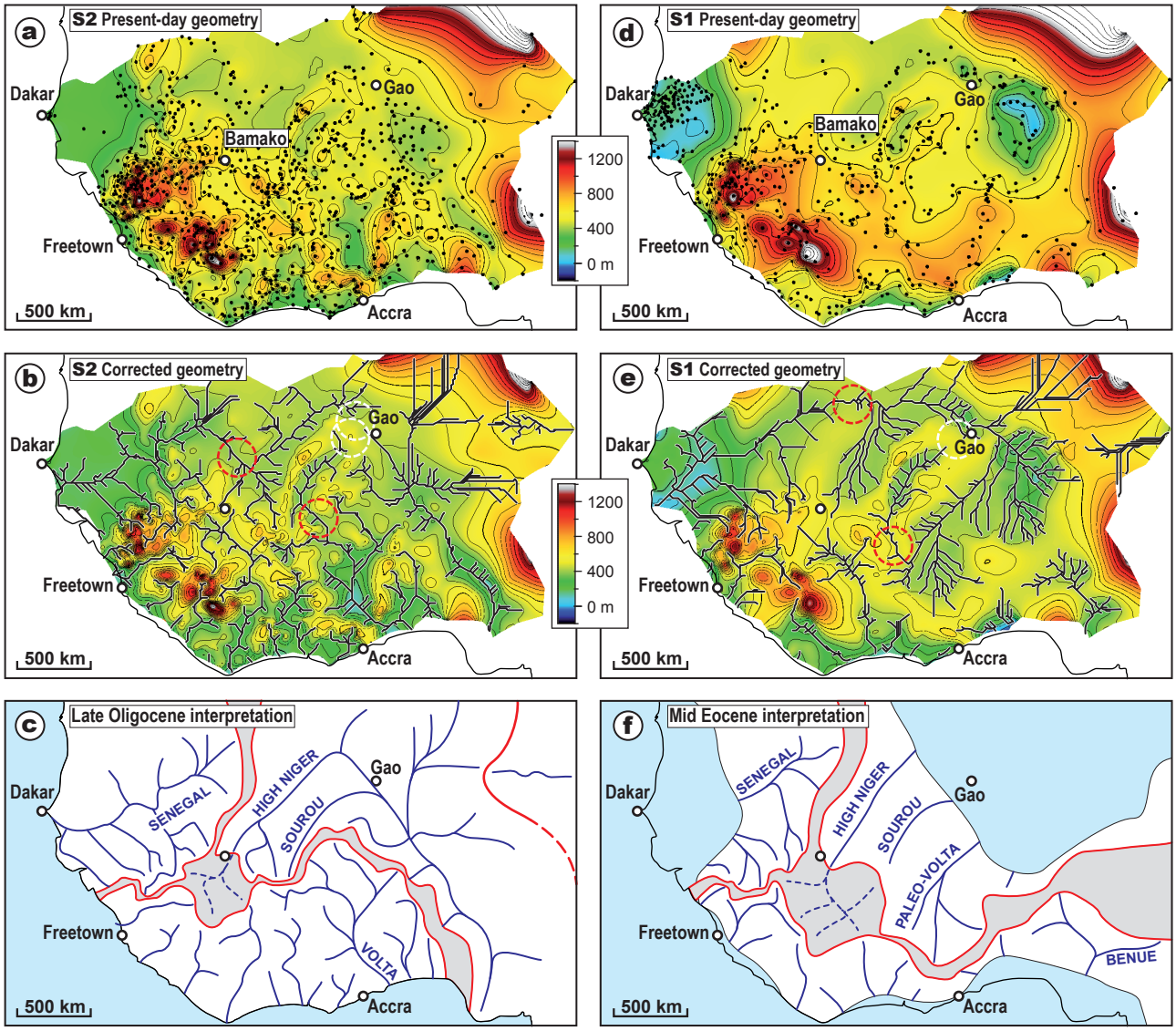

Chardon et al., Figure 7

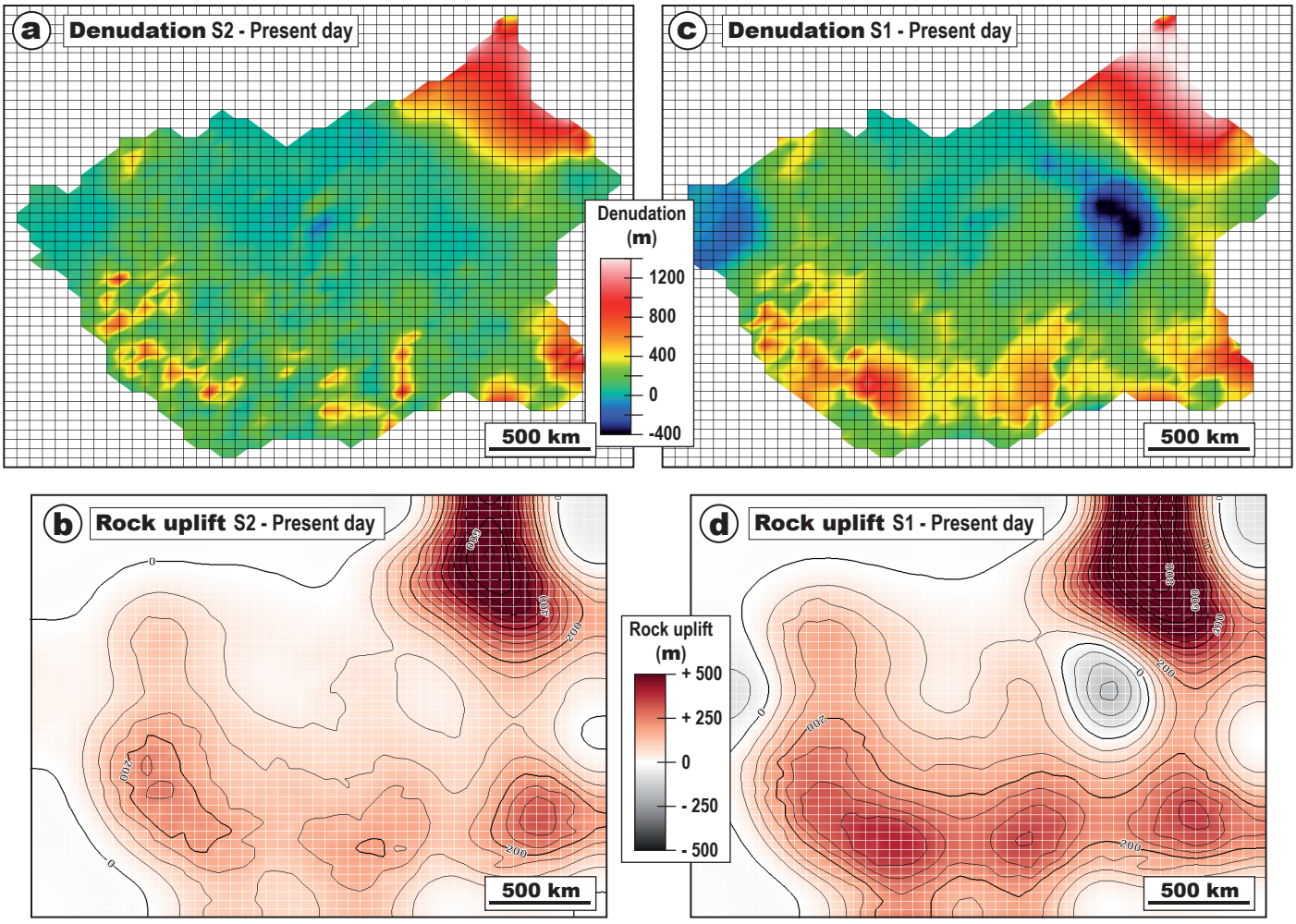

Chardon et al., Figure 8

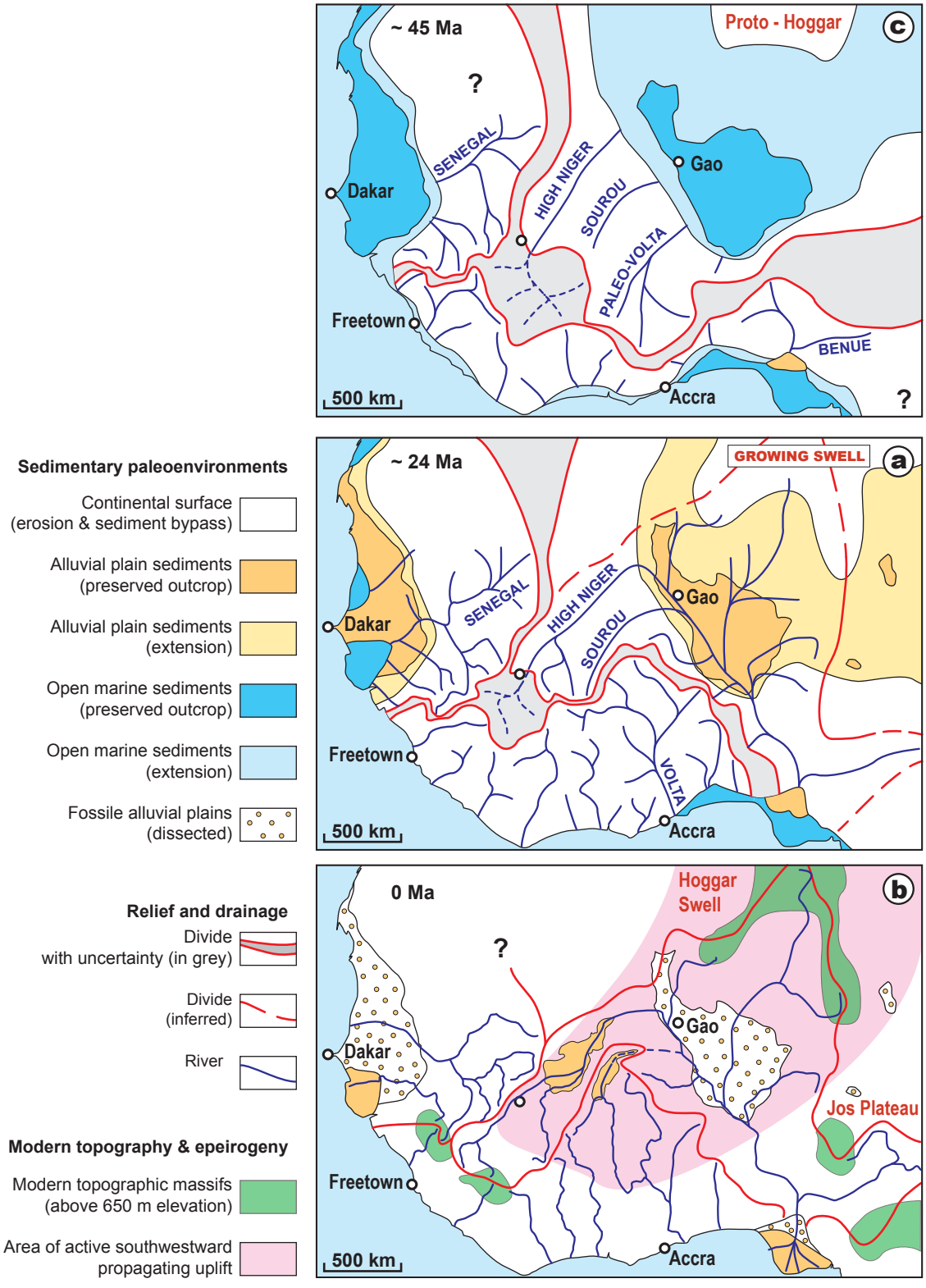

Chardon et al., Fig. 9

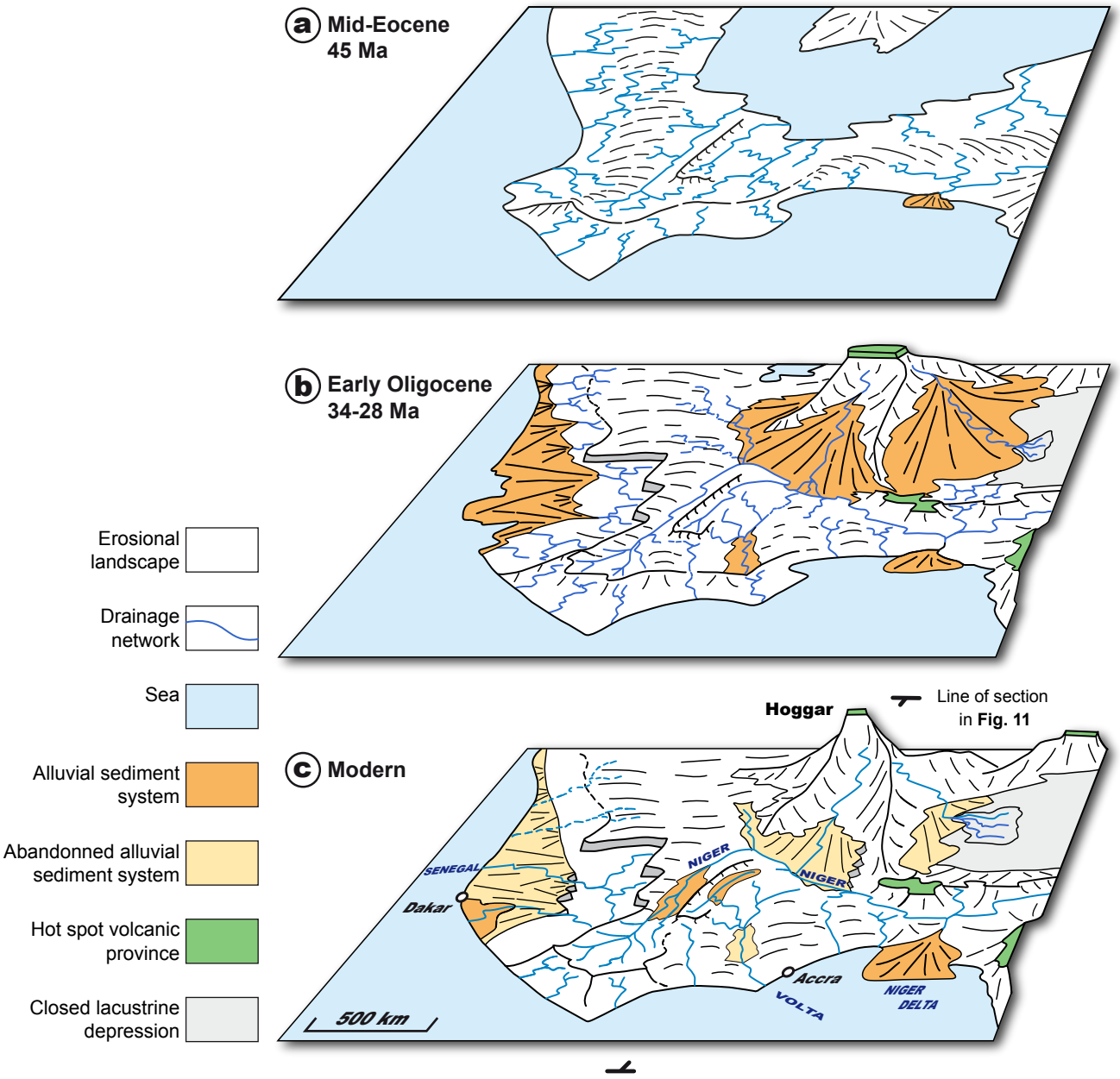

Chardon et al., Figure 10

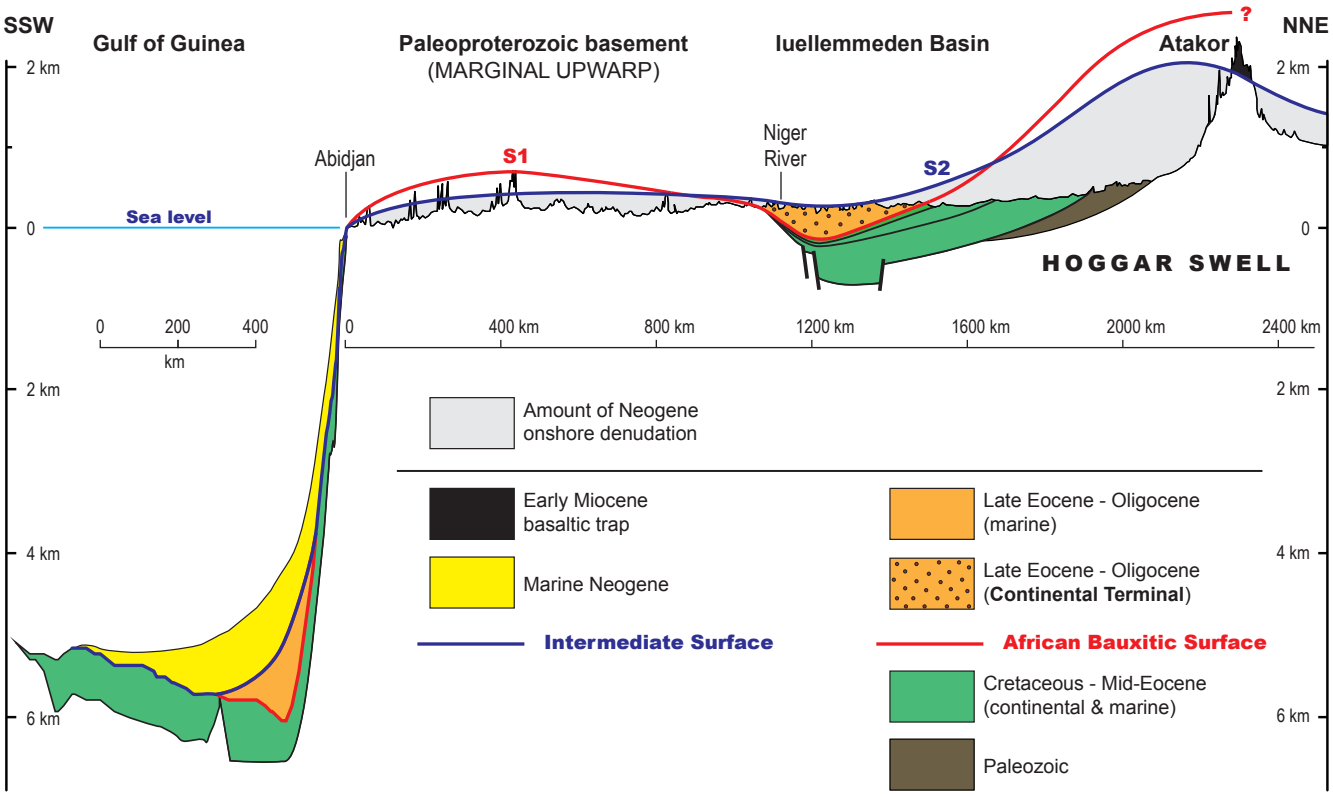

Chardon et al., Figure 11